



Electron scattering and nonlinear trapping by oblique whistler waves: The critical wave intensity for nonlinear effects

A. V. Artemyev, A. A. Vasiliev, D. Mourenas, O. V. Agapitov, V. V. Krasnoselskikh

► To cite this version:

A. V. Artemyev, A. A. Vasiliev, D. Mourenas, O. V. Agapitov, V. V. Krasnoselskikh. Electron scattering and nonlinear trapping by oblique whistler waves: The critical wave intensity for nonlinear effects. *Physics of Plasmas*, 2014, 21 (10), 102903 - 10 p. 10.1063/1.4897945 . insu-01171246

HAL Id: insu-01171246

<https://insu.hal.science/insu-01171246>

Submitted on 20 May 2016

HAL is a multi-disciplinary open access archive for the deposit and dissemination of scientific research documents, whether they are published or not. The documents may come from teaching and research institutions in France or abroad, or from public or private research centers.

L'archive ouverte pluridisciplinaire **HAL**, est destinée au dépôt et à la diffusion de documents scientifiques de niveau recherche, publiés ou non, émanant des établissements d'enseignement et de recherche français ou étrangers, des laboratoires publics ou privés.

Electron scattering and nonlinear trapping by oblique whistler waves: The critical wave intensity for nonlinear effects

A. V. Artemyev, A. A. Vasiliev, D. Mourenas, O. V. Agapitov, and V. V. Krasnoselskikh

Citation: *Physics of Plasmas* **21**, 102903 (2014); doi: 10.1063/1.4897945

View online: <http://dx.doi.org/10.1063/1.4897945>

View Table of Contents: <http://scitation.aip.org/content/aip/journal/pop/21/10?ver=pdfcov>

Published by the [AIP Publishing](#)

Articles you may be interested in

[Laboratory studies of nonlinear whistler wave processes in the Van Allen radiation belts](#)

Phys. Plasmas **22**, 091503 (2015); 10.1063/1.4928944

[Frequency sweep rates of rising tone electromagnetic ion cyclotron waves: Comparison between nonlinear theory and Cluster observation](#)

Phys. Plasmas **21**, 122309 (2014); 10.1063/1.4905065

[Nonlinear electron acceleration by oblique whistler waves: Landau resonance vs. cyclotron resonance](#)

Phys. Plasmas **20**, 122901 (2013); 10.1063/1.4836595

[Nonlinear electron motion in a coherent whistler wave packet](#)

Phys. Plasmas **15**, 073506 (2008); 10.1063/1.2959121

[Precipitation of trapped relativistic electrons by amplified whistler waves in the magnetosphere](#)

Phys. Plasmas **14**, 062903 (2007); 10.1063/1.2743618



PFEIFFER VACUUM

VACUUM SOLUTIONS FROM A SINGLE SOURCE

Pfeiffer Vacuum stands for innovative and custom vacuum solutions worldwide, technological perfection, competent advice and reliable service.

Electron scattering and nonlinear trapping by oblique whistler waves: The critical wave intensity for nonlinear effects

A. V. Artemyev,^{1,a)} A. A. Vasiliev,¹ D. Mourenas,² O. V. Agapitov,^{3,b)}
 and V. V. Krasnoselskikh²

¹*Space Research Institute, RAS, Moscow, Russia*

²*LPC2E/CNRS—University of Orleans, Orleans, France*

³*Space Sciences Laboratory, University of California, Berkeley, California 94720, USA*

(Received 11 August 2014; accepted 30 September 2014; published online 16 October 2014)

In this paper, we consider high-energy electron scattering and nonlinear trapping by oblique whistler waves via the Landau resonance. We use recent spacecraft observations in the radiation belts to construct the whistler wave model. The main purpose of the paper is to provide an estimate of the critical wave amplitude for which the nonlinear wave-particle resonant interaction becomes more important than particle scattering. To this aim, we derive an analytical expression describing the particle scattering by large amplitude whistler waves and compare the corresponding effect with the nonlinear particle acceleration due to trapping. The latter is much more rare but the corresponding change of energy is substantially larger than energy jumps due to scattering. We show that for reasonable wave amplitudes ~ 10 – 100 mV/m of strong whistlers, the nonlinear effects are more important than the linear and nonlinear scattering for electrons with energies ~ 10 – 50 keV. We test the dependencies of the critical wave amplitude on system parameters (background plasma density, wave frequency, etc.). We discuss the role of obtained results for the theoretical description of the nonlinear wave amplification in radiation belts. © 2014 AIP Publishing LLC.

[<http://dx.doi.org/10.1063/1.4897945>]

I. INTRODUCTION

The resonant interaction of electrons with whistler-mode waves plays an important role in electron scattering and acceleration in many plasma systems: radiation belts,^{26,50} solar wind,^{20,28} shock waves,^{56,58} and planetary magnetotails.^{27,40} The general approach for the description of such an interaction is based on the quasi-linear theory of charged particle scattering by uncorrelated small amplitude waves.^{18,25,55} The alternative approach corresponding to the consideration of the wave-particle nonlinear interaction^{42,53} is generally applied for systems with high enough wave amplitudes.^{1,11,14,35,39,48} This approach is based on the analysis of nonlinear equations of the charged particle motion.^{10,19,23,34} The dynamical system approach can also be applied for analysis of such systems.³⁸ Almost all the modern global three-dimensional models describing the evolution of an ensemble of charged particles resonantly interacting with whistler waves take into account only quasi-linear effects of scattering and do not include any nonlinear effects (see review in Ref. 45 and references therein).

Recently, spacecraft observations in the Earth radiation belts,^{12,13,30} at the bow-shock,^{21,57} and in the magnetotail^{16,29} suggest that a significant part of the whistler wave population actually consists of high-amplitude waves. The electron resonant interaction with such waves can have a nonlinear character, including effects of electron trapping. Thus, the possible role of these nonlinear effects for large electron ensembles is at this time an open and pressing question.^{3,54}

The character of the wave-particle resonant interaction is determined by the competition of two factors: wave intensity and inhomogeneity of the background magnetic field.^{24,34} For strong enough wave amplitude, the resonant interaction is nonlinear with a possible particle trapping. The threshold on the wave amplitude necessary for particle trapping was found for several systems with various wave-modes.^{1,9,37} However, the possibility of particle trapping and its subsequent nonlinear acceleration does not necessarily means that this process plays an important role in realistic systems. In fact, particle trapping is a probabilistic process,^{4,22,43} i.e., only a small portion of resonant particles can be trapped by a wave during the first resonant interaction, while other resonant particles should be scattered. A probability of trapping (ratio of trapped particles to the total amount of resonant particles) can be defined for each particular system. For relativistic electron interaction with oblique whistler waves, the probability of trapping was calculated and numerically tested for both Landau and cyclotron resonances (see Refs. 5 and 6). Thus, these probabilities can be used to estimate the relative impact of nonlinear trapping in particle acceleration. This impact can be either small (when particles are so rarely trapped that the much more frequent scattering is globally more effective at changing particle energy) or large (when the change of particle energy due to trapping is so large as compared to changes due to scattering that even a small probability of trapping results in a more effective nonlinear acceleration). Moreover, in some particular situations a general balance could be reached between scattering and trapping, with both processes playing comparable roles in particle acceleration/deceleration. In the following, we address the preceding questions in the case of

^{a)}Electronic mail: ante0226@gmail.com

^{b)}Also at National Taras Shevchenko University of Kiev, Kiev, Ukraine.

electron resonant interaction with oblique whistler-mode waves. First, we derive the relevant equations describing nonlinear electron scattering and trapping, which then allows us to compare in details these two processes.

II. MAIN EQUATIONS

We consider the interaction of relativistic electrons (with rest mass m_e and charge— e) with a strong oblique whistler wave described by the scalar potential $\Phi = \Phi_0 \sin \phi$ with phase ϕ . We focus on the Landau resonance and, as a result, can assume the conservation of the magnetic moment of particles (i.e., the corresponding wave phase does not depend on the coordinate transverse to the background magnetic field). The model of the magnetic field⁸ is chosen so that after averaging over electron gyrorotation, the magnetic field magnitude $B(z)$ depends only on the coordinate z along field lines (i.e., this magnetic field model does not include any effect of curvature of field lines). In this case, the Hamiltonian system describing the Landau resonant interaction of an electron and quasi-electrostatic wave can be written as

$$\begin{aligned} H &= \gamma - \varepsilon u_0(z) \sin \phi, \\ \gamma &= \sqrt{1 + p_z^2 + \xi b(z)}, \\ \phi &= \phi_0 + \int_{\phi_0}^z k_{\parallel}(z') dz' - \omega t. \end{aligned} \quad (1)$$

In system (1), we use dimensionless variables: particle parallel momentum p_z is normalized on $m_e c$; the coordinate z is normalized on R_0 (here, $R_0 = R_E L$ is the scale of the background magnetic field inhomogeneity, L denotes the L -shell, while R_E is the Earth radius); the background magnetic field is normalized to its equatorial value $b(z) = B(z)/B_0$; the dimensionless magnetic moment is $\xi = (\gamma_0^2 - 1) \sin^2 \alpha_0$, where γ_0 and α_0 are initial electron gamma factor and equatorial pitch-angle; wavenumber is normalized as $(k_{\parallel}, k_{\perp}) \rightarrow (k_{\parallel}, k_{\perp}) R_0$; the normalized wave frequency is $\omega \rightarrow \omega R_0 / c = \omega_m \chi$, where $\omega_m = \omega m_e c / e B_0$ and $\chi = e B_0 R_0 / m_e c^2$; the wave amplitude is normalized as $e \Phi_0 / m_e c^2 = \varepsilon u_0(z)$, where $u_0(z) = u(z) J_0(\eta)$ and function $u(z) \in [0, 1]$ describes the distribution of the wave amplitude along field lines (this distribution is derived from the statistics of spacecraft observations, see details in Ref. 5), while $J_0(\eta)$ is the Bessel function of the first order with the argument $\eta = (k_{\perp} / \chi) \sqrt{\xi / b(z)}$; and ϕ_0 is the initial wave phase. In contrast to several previous studies,^{5,15,49} we consider the wave-particle interaction for a coherent monochromatic wave occupying the entire flux tube with a given amplitude profile. This simplification allows us to reduce a number of free parameters. Effects of a finite-length of a wave packet should be considered further.

The pair of conjugate variables in Eq. (1) is (z, p_z) . Thus, the corresponding Hamiltonian equations have a form

$$\begin{aligned} \dot{p}_z &= -\frac{1}{2\gamma} \xi b' + \varepsilon k_{\parallel} u_0 \cos \phi, \\ \dot{z} &= p_z / \gamma, \end{aligned} \quad (2)$$

where $' = d/dz$. To consider the resonant wave-particle interaction, we rewrite Eq. (2) in terms of wave-phase along the particle trajectory

$$\begin{aligned} \dot{\phi} &= \frac{k_{\parallel} p_z}{\gamma} - \omega, \\ \gamma &= \sqrt{\frac{1 + \xi b}{1 - (\dot{\phi} + \omega)^2 / k_{\parallel}^2}}. \end{aligned} \quad (3)$$

We take one additional derivative of the first equation from system (3) to obtain the equation for $\ddot{\phi}$,

$$\ddot{\phi} = \frac{k'_{\parallel} p_z}{\gamma} \dot{z} + \frac{k_{\parallel} \dot{p}_z}{\gamma} - \frac{k_{\parallel} p_z}{\gamma^2} \dot{\gamma}. \quad (4)$$

We substitute Eqs. (2) and (3) into Eq. (4) to get

$$\begin{aligned} \frac{\ddot{\phi}}{1 - (\dot{\phi} + \omega)^2 / k_{\parallel}^2} &= k'_{\parallel} \frac{(\dot{\phi} + \omega)^2}{k_{\parallel}^2} + \frac{k_{\parallel} \dot{p}_z}{\gamma} \\ &\quad - \frac{1}{2} \frac{\xi b'(z)}{1 + \xi b(z)} \frac{(\dot{\phi} + \omega)^2}{k_{\parallel}} \\ &\quad + \frac{(\dot{\phi} + \omega)^2 / k_{\parallel}^2}{1 - (\dot{\phi} + \omega)^2 / k_{\parallel}^2} \frac{k'_{\parallel} (\dot{\phi} + \omega)^2}{k_{\parallel}}, \end{aligned} \quad (5)$$

where \dot{p}_z should be substituted from Eq. (2). Considering the above equation in the vicinity of the Landau resonance $\dot{\phi} = 0$ gives

$$\frac{\ddot{\phi}}{k_{\parallel}} = \frac{k'_{\parallel}}{k_{\parallel}} v_R^2 - \frac{\xi b'}{2\gamma^2} + \frac{k_{\parallel} \varepsilon u_0}{\gamma \gamma_R^2} \cos \phi, \quad (6)$$

where $v_R(z) = \omega / k_{\parallel}(z)$ and

$$\begin{aligned} \gamma_R &= 1 / \sqrt{1 - v_R^2}, \\ \gamma &= \gamma_R \sqrt{1 + \xi b}. \end{aligned} \quad (7)$$

In Eq. (6), the phase ϕ changes much faster than the position on the z -axis: $\dot{\phi} \sim k_{\parallel} \gg 1$. Thus, following to Ref. 23 we can consider Eq. (6) as an equation for ϕ with z as a slowly varying parameter. In this case, Eq. (6) can be rewritten in a form

$$\dot{P} = -\frac{\gamma_R^2}{2\gamma k_{\parallel}} \left(\xi b' - 2\gamma^2 \frac{k'_{\parallel}}{k_{\parallel}} v_R^2 \right) + \varepsilon u_0 \cos \phi, \quad (8)$$

where we introduce $P = \gamma \gamma_R^2 \dot{\phi} / k_{\parallel}$. It can be shown that P and ϕ are conjugate variables for the Hamiltonian H_{ϕ} (see Appendix A in Ref. 6)

$$H_{\phi} = \frac{1}{2} \frac{k_{\parallel}^2}{\gamma_R^2 \gamma} P^2 + D(z) \phi - \varepsilon u_0 \sin \phi, \quad (9)$$

where

$$\begin{aligned} D(z) &= \frac{\gamma_R^2}{2\gamma k_{\parallel}} \left(\xi b' - 2\gamma^2 \frac{k'_{\parallel}}{k_{\parallel}} v_R^2 \right), \\ U_{\phi}(z) &= D(z) \phi - \varepsilon u_0(z) \sin \phi. \end{aligned} \quad (10)$$

The effective potential energy U_ϕ of Hamiltonian (9) depends via the z coordinate on both the wave intensity variation along field line and the magnetic field inhomogeneity. Phase portraits of Hamiltonian (9) for three cases $D > \varepsilon u_0$, $D = \varepsilon u_0$, and $D < \varepsilon u_0$ are displayed in Fig. 1. The presence of a region with closed trajectories in the case with $D < \varepsilon u_0$ corresponds to a possible particle trapping.⁴ This effect is considered in Sec. IV. However, trapping is a probabilistic process—i.e., each passage through resonance does not result in trapping. If trapping is not realized, the particle is scattered at resonance with the wave. Moreover, for the system with $D > \varepsilon u_0$, only scattering is possible. We treat this effect in Sec. III.

III. SCATTERING

In this section, we consider the evolution of particle energy in the vicinity of resonance in the case when a particle is not trapped by the wave. Particle momentum P is only slightly changed by scattering at the resonance crossing.^{32,33} This change can be found from Eq. (8)

$$\Delta P = \int_{-\infty}^{t^*} \dot{P} dt = 2\varepsilon u_0(z) \int_{-\infty}^{\phi^*} \frac{\cos \phi d\phi}{\dot{\phi}}, \quad (11)$$

where t^* and ϕ^* are time moment and phase at resonance. We use $\dot{\phi} = P k_{\parallel}^2 / \gamma \gamma_R^2$ and Eq. (9) to rewrite Eq. (11) as

$$\Delta P = \varepsilon u_0 \sqrt{\frac{2\gamma \gamma_R^2}{k_{\parallel}^2}} \int_{-\infty}^{\phi^*} \frac{\cos \phi d\phi}{\sqrt{H_\phi - D\phi + \varepsilon u_0 \sin \phi}}. \quad (12)$$

The resonant phase ϕ^* is defined from the equation $\dot{\phi} = 0$. The particle Hamiltonian H_ϕ can be written at resonance ($\phi = \phi^*$, $P = 0$). Thus, we can rewrite Eq. (12) in a form

$$\begin{aligned} \Delta P &= \varepsilon u_0 \sqrt{\frac{2\gamma \gamma_R^2}{k_{\parallel}^2}} \int_{-\infty}^{\phi^*} \frac{\cos \phi d\phi}{\sqrt{D\phi^* - \varepsilon u_0 \sin \phi^* - D\phi + \varepsilon u_0 \sin \phi}} \\ &= \varepsilon u_0 \sqrt{\frac{2\gamma \gamma_R^2}{k_{\parallel}^2 D}} \int_{-\infty}^{\phi^*} \frac{\cos \phi d\phi}{\sqrt{2\pi\theta - \phi + a \sin \phi}} \\ &= \varepsilon u_0 \sqrt{\frac{2\gamma \gamma_R^2}{k_{\parallel}^2 D}} f(\theta, a), \end{aligned} \quad (13)$$

where $a = \varepsilon u_0 / D$, $\theta = (\phi^* - a \sin \phi^*) / 2\pi$, and ϕ^* is defined by the equation $2\pi\theta - \phi^* + a \sin \phi^* = 0$. The function $f(\theta, a)$ is shown in Fig. 2 for different values of a . One can see that f is a periodic function of θ . The value of θ is determined by the exact value of the fast oscillating phase ϕ at

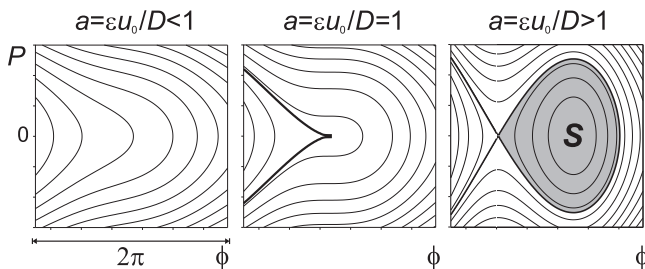


FIG. 1. Phase portraits of system (9).

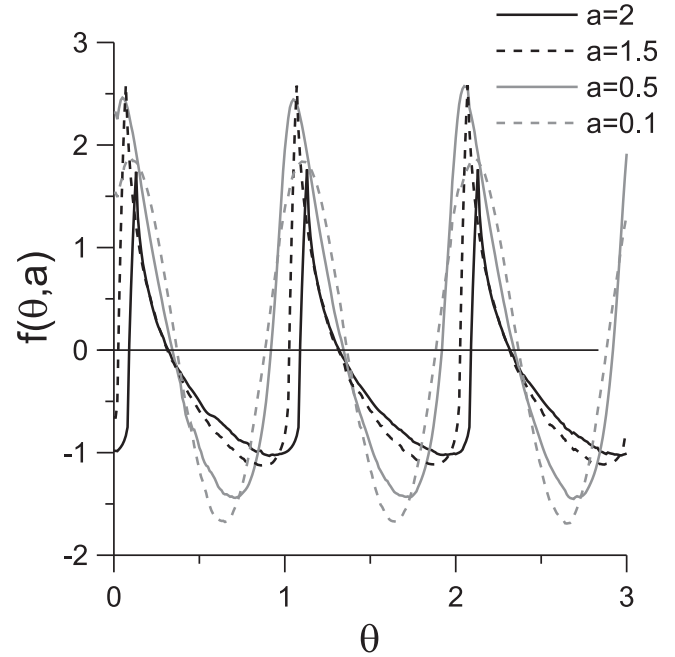


FIG. 2. Profiles of $f(\theta, a)$ function for four values of a .

resonance. Thus, θ can be assumed to be a random variable with uniform distribution over $\theta \in [0, 1]$ (see Refs. 4, 32, and 33). In this case, we can consider the average value of ΔP and the corresponding dispersion $\text{Var}(\Delta P)$ around this average

$$\langle \Delta P \rangle = \varepsilon u_0 \sqrt{\frac{2\gamma \gamma_R^2}{k_{\parallel}^2 D}} \langle f(\theta, a) \rangle_\theta = P_0 \langle f \rangle_\theta,$$

$$\text{Var}(\Delta P) = \langle \Delta P^2 \rangle - \langle \Delta P \rangle^2 = P_0^2 \left(\langle f^2 \rangle_\theta - \langle f \rangle_\theta^2 \right). \quad (14)$$

Both terms ΔP and $\text{Var}(\Delta P)$ are shown in Fig. 3 as functions of a . For $a < 1$ we have $\langle P \rangle = 0$, while for $a > 1$ there is a finite regular drift of P (i.e., $\langle P \rangle \neq 0$). Since P is a function of γ , the preceding expressions for $\langle P \rangle$ and $\text{Var}(\Delta P)$ can be rewritten under the form of corresponding expressions for

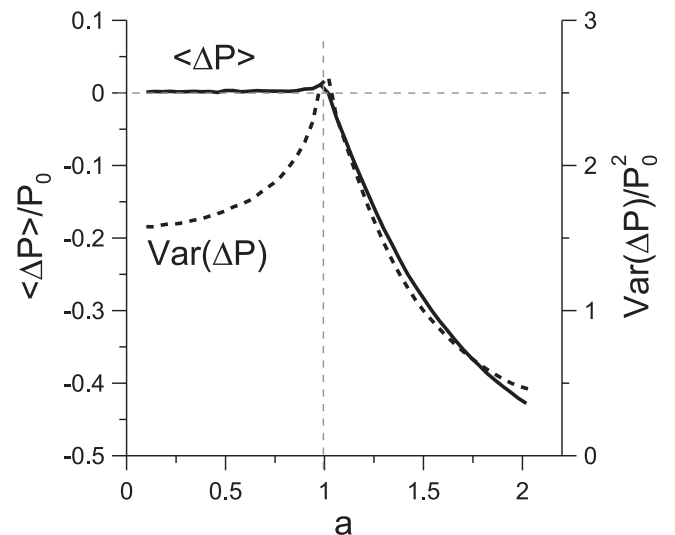


FIG. 3. ΔP and $\text{Var}(\Delta P)$ as functions of a .

the mean and variance of the particle energy (γ). To this aim, we rewrite ΔP in a form

$$\Delta P = \frac{\gamma \gamma_R^2}{k_{\parallel}^2} \Delta \dot{\phi} = \frac{\gamma \gamma_R^2}{k_{\parallel}^2} \left(\frac{k_{\parallel} \Delta p_z}{\gamma} - \frac{k_{\parallel} p_z}{\gamma} \frac{\Delta \gamma}{\gamma} \right). \quad (15)$$

We can use $\Delta \gamma = p_z \Delta p_z / \gamma$ and $p_z / \gamma = v_R$ to rewrite Eq. (15) as

$$\Delta \gamma = v_R k_{\parallel} \Delta P. \quad (16)$$

Thus, we can substitute Eq. (16) into Eq. (14) to finally get the relevant expressions for mean energy change and variance

$$\begin{aligned} \langle \Delta \gamma \rangle &= \Upsilon_0 \langle f \rangle_{\theta}, \\ \text{Var}(\Delta \gamma) &= \Upsilon_0^2 \left(\langle f^2 \rangle_{\theta} - \langle f \rangle_{\theta}^2 \right), \\ \Upsilon_0 &= v_R k_{\parallel} P_0 = \frac{2 v_R \gamma \epsilon k_{\parallel} u_0}{\sqrt{k_{\parallel} \xi b' - 2 \gamma^2 k_{\parallel}^2 v_R^2}}, \end{aligned} \quad (17)$$

where all variables (except for the dimensionless magnetic moment ξ) must be calculated at the position of resonance $z = z_R$, so that Υ_0 is a function of z_R .

To demonstrate the effect of charged particle scattering at the resonance, we consider the particular case of a wave propagating at the Gendrin angle: $k_{\parallel} = k_0 / b(z)$; with $k_0 = 2 \omega_{pe} \omega$, and ω_{pe} is the ratio of plasma frequency and electron gyrofrequency at the equator (see details on this approximation for k_{\parallel} in Ref. 6). For the Earth radiation belts ω_{pe} is a function of L -shell.⁴¹ In this case, Eq. (17) takes a form

$$\begin{aligned} \Upsilon_0 &= \frac{1}{\sqrt{k_0 b'}} \frac{2 v_R \gamma u_0 k_0 \epsilon}{\sqrt{\xi b + 2 \gamma^2 v_R^2}}, \\ a &= \frac{\epsilon u_0}{D} = \frac{1}{\gamma_R^2 b'} \frac{2 \gamma u_0 k_0 \epsilon}{\xi b + 2 \gamma^2 v_R^2}. \end{aligned} \quad (18)$$

Here, factor $k_0 \epsilon = e E_{0\parallel} R_0 / m_e c^2$ is about one for high-amplitude waves ($E_{0\parallel} = \Phi_0 k_0$ is the electric field amplitude), while factor $\sim 1 / \sqrt{k_0} \ll 1$ determines the smallness of the energy change for a single passage through the resonance. The position of the resonance z_R is determined by the equation $\gamma_0 = \gamma_R(z_R) \sqrt{1 + \xi b(z_R)}$, where γ_0 is the initial particle energy. Thus, the resonance location z_R depends on γ_0 and equatorial pitch-angle α_0 . For various initial energies (γ_0), we have determined $z_R(\alpha_0)$ and plotted Υ_0 as a function of α_0 in Fig. 4, using the same wave and plasma parameters as in Ref. 5. The decrease of the particle energy corresponds to a shrinking range of α_0 where $\Upsilon_0 \neq 0$. The absolute value of Υ_0 is about $k_0 \epsilon / \sqrt{k_0}$. The mean energy change is

proportional to $\Upsilon_0 \sim u_0 k_0 \epsilon / \sqrt{k_0}$ at small equatorial pitch-angle $\alpha_0 < 45^\circ$ where it becomes independent of α_0 . There it increases with decreasing energy in Fig. 4, due to a general increase of wave intensity $u_0(z_R)$ as latitude of resonance is reduced for a realistic latitudinal distribution of oblique wave intensity based on satellite measurements (see Ref. 5).

To further examine the effect of scattering, we numerically integrate Eq. (2) for two trajectories. The first trajectory corresponds to initial $\alpha_0 = 10^\circ$. In this case, the averaged $\langle \Delta \gamma \rangle$ is equal to zero and we should obtain only random jumps of γ with the average amplitude $\sim \sqrt{\text{Var}(\Delta \gamma)}$. This trajectory is displayed in the top panels of Fig. 5. Particle oscillations between mirror points correspond to a closed trajectory in the (z, p_z) plane. At the resonance $z_R \approx 0.625$, the particle experiences jumps in energy and scattering of z and p_z values. The corresponding energy jumps are randomly negative or positive, with an average jump amplitude close to the theoretical prediction (see the right top panel in Fig. 5).

The second trajectory (bottom panels in Fig. 5) is integrated with an initial $\alpha_0 = 60^\circ$. In this case, the variance $\sim \sqrt{\text{Var}(\Delta \gamma)}$ is substantially smaller than the mean $\langle \Delta \gamma \rangle$. Thus, at each passage through resonance the scattering of the particle should correspond to a decrease of its energy due to $\langle \Delta \gamma \rangle < 0$. Indeed, one can see in the right bottom panel in Fig. 5 this expected behavior (decrease) of γ .

Although the integration of individual particle trajectories already shows a good agreement between numerical results and analytical estimates, a more comprehensive check of Eq. (17) requires to consider a large particle ensemble. In this case, random fluctuations can be averaged and mean values of $\text{Var}(\Delta \gamma)$, $\langle \Delta \gamma \rangle$ can be obtained numerically as functions of the initial energy and pitch-angle. Results of such massive tests are shown in Fig. 6 for three energies and two values of the wave-amplitude. Each point (symbol) in Fig. 6 corresponds to an averaged value obtained by integration of 10^4 particle trajectories. One can see that all dependencies (resonant latitude λ corresponding to z_R , $\text{Var}(\Delta \gamma)$, and $\langle \Delta \gamma \rangle$) on the initial particle pitch-angle are well reproduced. It demonstrates that the analytical approximations given by Eq. (17) can be safely used to describe the behavior of large particle ensembles.

IV. TRAPPING

Particle trapping by quasi-electrostatic whistler-mode waves into the Landau resonance was described in details in Refs. 5 and 6. Here, we reproduce the main results, to compare the efficiency of trapping and scattering processes. An example of particle trajectory with trapping of particle by the

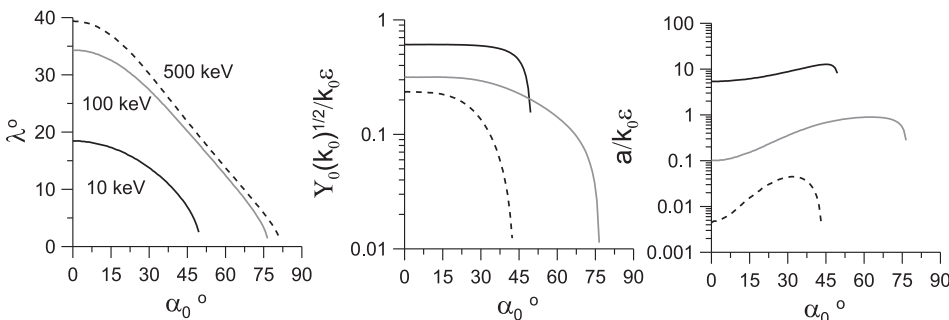


FIG. 4. Resonant latitude, normalized Υ_0 , and a as functions of α_0 for three values of electron energy.

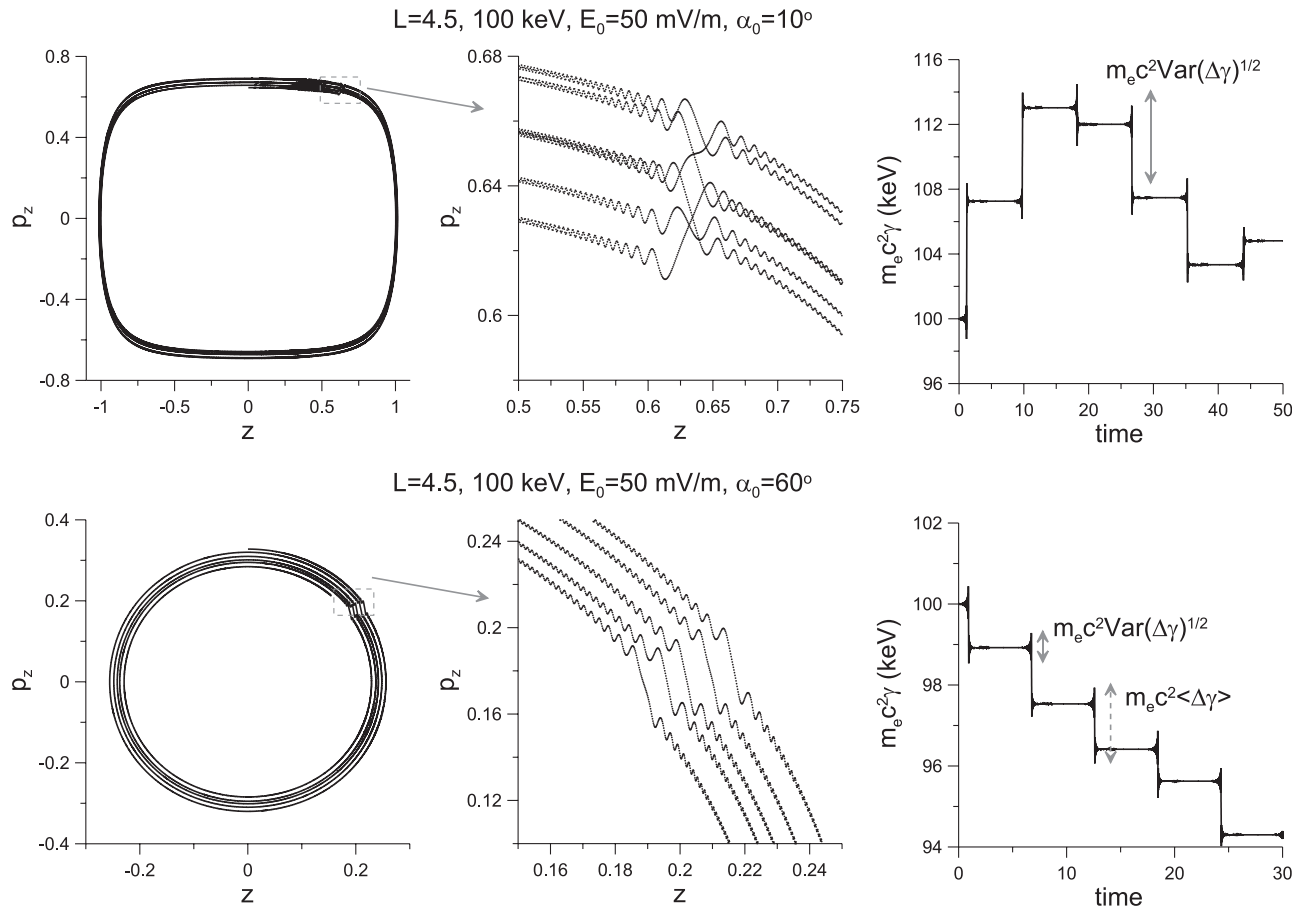


FIG. 5. Two test trajectories with scattering: trajectories in (z, p_z) plane, fragments of trajectories with scattering, and energy as a function of time.

wave is shown in Fig. 7. This trajectory is obtained by numerical integration of system (1) with the same parameters as used for the trajectory shown in Fig. 5 (bottom panels), but with a two times larger wave amplitude. Initially, the particle oscillates between mirror points (bounce oscillations) and after a certain time, it becomes trapped by the wave. The trapped particle moves with the wave to higher latitude and is strongly accelerated. One trapping-escape event results in an energy gain about 70 keV in accordance with previous estimates.^{5,6,39}

In contrast to scattering, the probability of particle trapping is small: only some limited portion of particles passing through the resonance becomes trapped.^{4,33} The ratio of the number of trapped particles to the total number of particles passed through the resonance can be called a probability of trapping Π . An analytical expression for Π has been derived in Ref. 6 and tested numerically in Ref. 7. Over a realistic parameter range, Π is defined by the expression

$$\Pi = \frac{\sqrt{\varepsilon}}{4\pi\omega_{pe}k_{\parallel}D} \frac{\partial S}{\partial z}, \quad (19)$$

where the area S is shown by grey color in Fig. 1 and is defined by the equation

$$S = 2^{2/3} \gamma_R b \sqrt{u_0 \gamma} \int_{\phi_s}^{\phi_m} \sqrt{\frac{1}{a}(\phi_s - \phi) - \sin \phi_s + \sin \phi} d\phi, \quad (20)$$

where $\phi_s = -\arccos(1/a)$, ϕ_m is a root of the equation $(\phi_s - \phi) + a \sin \phi - a \sin \phi_s = 0$ different from ϕ_s (see details in Appendix A of Ref. 6).

V. SCATTERING VS. TRAPPING

For given initial particle pitch-angle α_0 and energy γ_0 , we can compare estimates of energy jumps due to scattering ΔE_{scat} and due to trapping ΔE_{trap} :

$$\begin{aligned} \Delta E_{scat} &= m_e c^2 (1 - \Pi) \sqrt{\langle \Delta \gamma \rangle^2 + \text{Var}(\Delta \gamma)}, \\ \Delta E_{trap} &= m_e c^2 \Pi \Delta \gamma_{trap}, \end{aligned} \quad (21)$$

where the expression for the energy jumps due to trapping $\sim \Delta \gamma_{trap}$ was derived in Ref. 6. The change $\Delta \gamma_{trap}$ can be defined as a difference of the particle gamma factors at the point of the escape from the resonance and initial value of γ . The ratio $\Delta E_{trap}/\Delta E_{scat}$ is shown in Fig. 8 for different particle energies and wave amplitudes. One can see that $\Delta E_{trap}/\Delta E_{scat}$ profiles look similar with Π profiles, i.e., the main variation with α_0 is provided by the probability variation with α_0 . For small energies ~ 10 keV, almost all the α_0 -range available for resonant interaction corresponds to a predominance of acceleration due to trapping. For larger electron energies, the available α_0 -range for resonance becomes shorter and only half of this range corresponds to $\Delta E_{trap}/\Delta E_{scat} > 1$. However, an increase of wave amplitude results

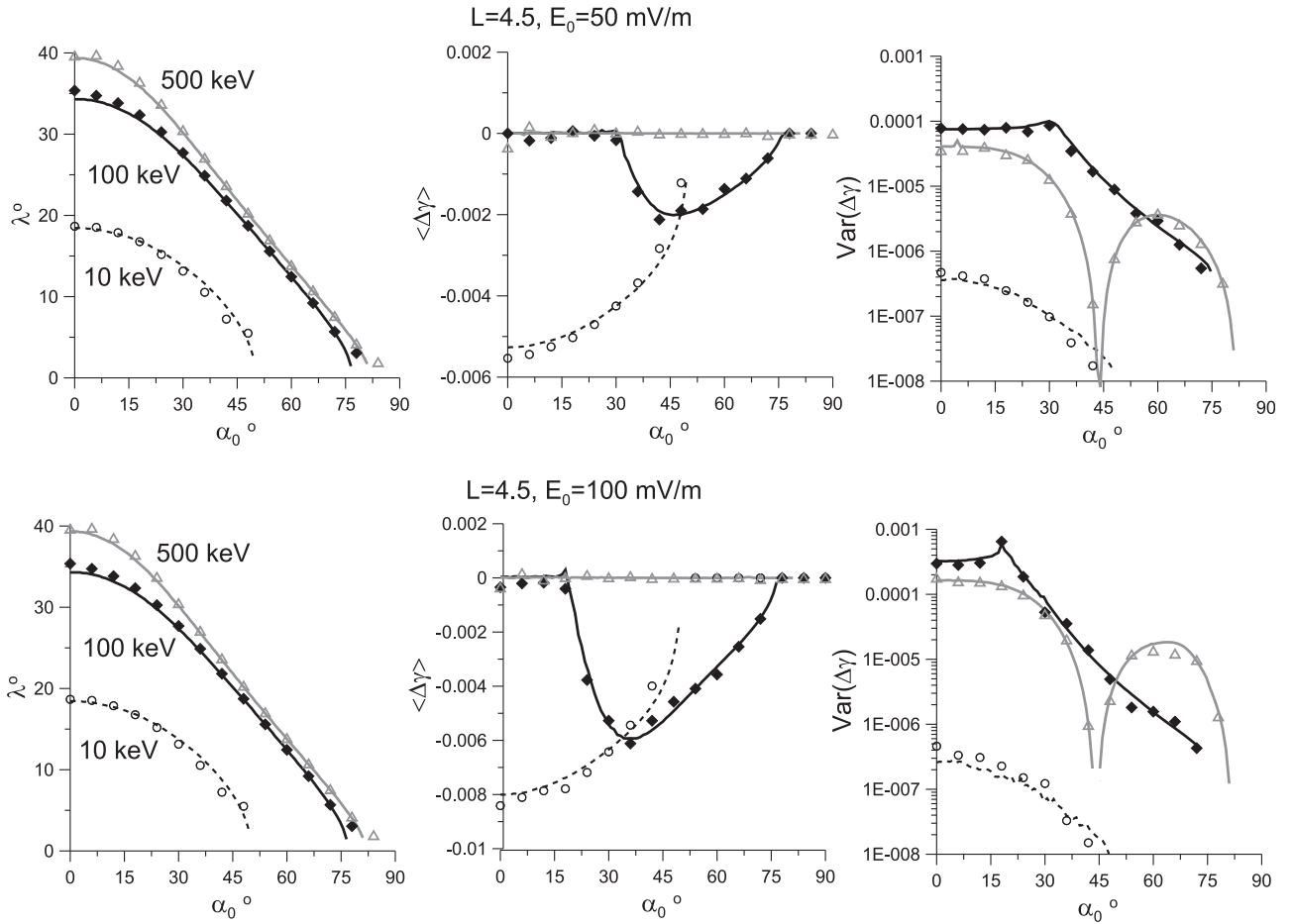


FIG. 6. Resonant latitudes, mean energy change, and variance of energy changes, as obtained from analytical expressions in Eq. (17) (curves) and by numerical simulations (symbols).

in a widening of the α_0 -range corresponding to $\Delta E_{trap}/\Delta E_{scat} > 1$. This effect is due to the increase of $\Delta\gamma_{trap}$ with wave amplitude ε (see Ref. 6), while the ratio Π/Υ_0 decreases with ε as $\Pi/\Upsilon_0 \sim \sqrt{\varepsilon}/\varepsilon \sim 1/\sqrt{\varepsilon}$.

For a given equatorial pitch-angle α_0 and energy γ_0 , one can further determine the critical value of the wave amplitude $E_{||0}^*$ such that changes in energy due to trapping exceed scattering-induced changes, i.e., such that $\Delta E_{trap} > \Delta E_{scat}$ for $E_{||0} > E_{||0}^*$. For several values of energy, the profiles $E_{||0}^*(\alpha_0)$

are shown in Fig. 9. First, we note that for any electron energy below 80 keV, there exists an α_0 -domain such that the corresponding value of $E_{||0}^*$ is rather small (< 25 mV/m). Waves with substantially larger amplitudes have often been observed in the radiation belts.^{1,12,13} However, the pitch-angle range where $E_{||0}^* < 100$ mV/m is really large (with a domain $0 \leq \alpha_0 \leq 45^\circ$) only for small particle energies ~ 10 keV. For larger energies, the range of α_0 where $E_{||0}^* < 100$ mV/m is only about 5° – 10° .

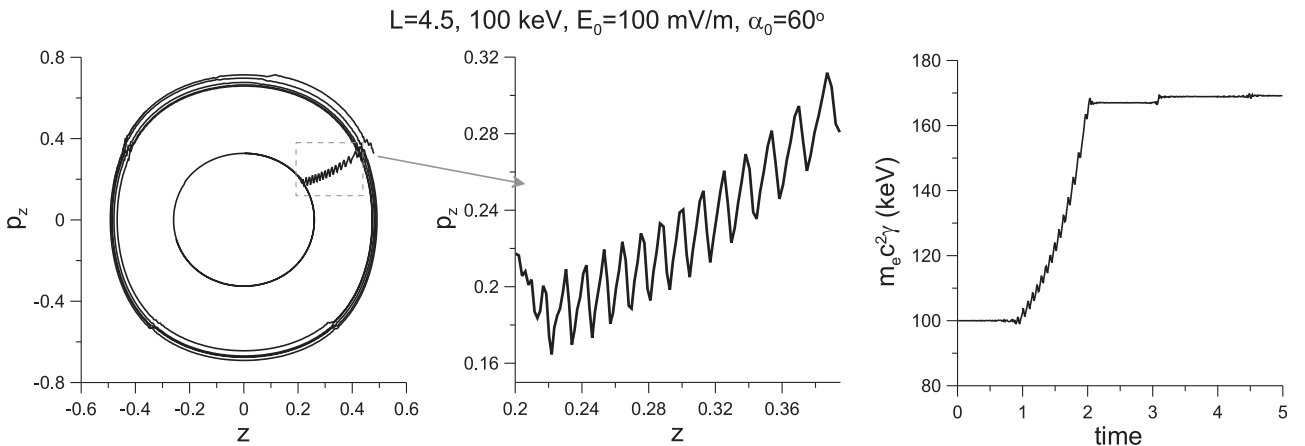


FIG. 7. Test trajectory with trapping: trajectory in (z, p_z) plane, fragments of trajectory with trapping, energy as a function of time.

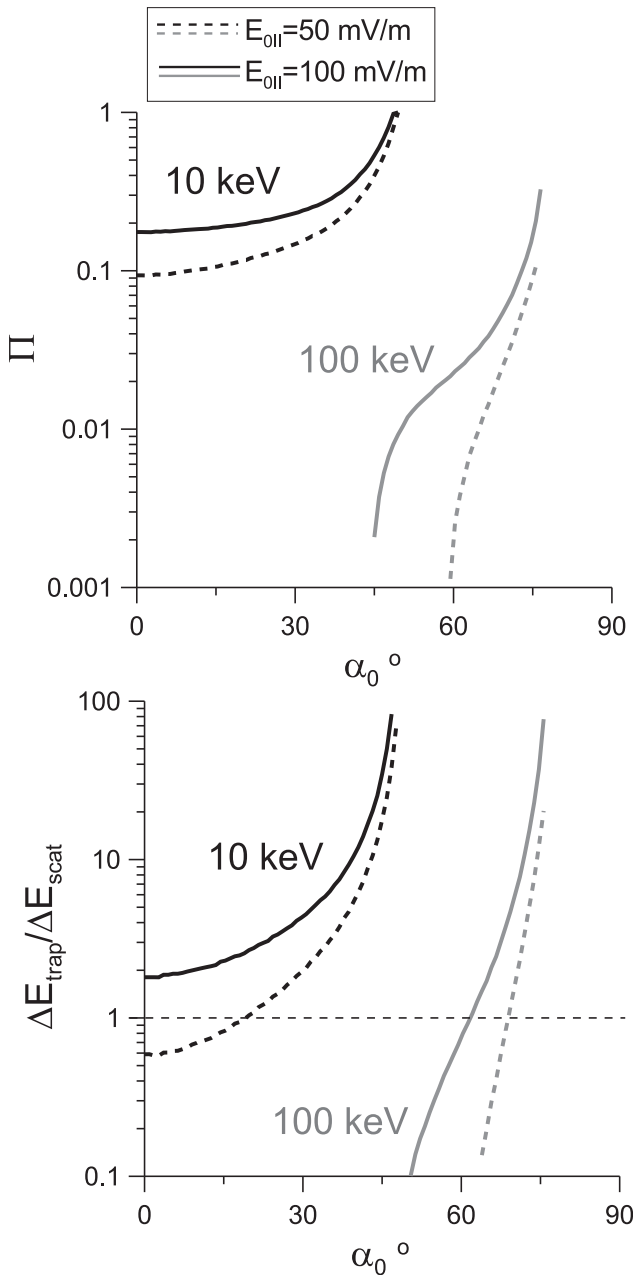


FIG. 8. Probability of trapping and ratio $\Delta E_{\text{trap}}/\Delta E_{\text{scat}} > 1$ for two energies and two wave amplitudes.

We can also infer from the above estimates that the increase of L -shell value (i.e., the increase of R_0 and ω_{pe} parameters) results in an increase of the critical wave amplitude. Thus, at larger L , a higher wave intensity is necessary for nonlinear acceleration to prevail. This is an interesting and important result, because previous studies have shown that the increase of the L -shell value should correspond to an increase of the efficiency of nonlinear acceleration, i.e., an increase of $\Delta\gamma_{\text{trap}}$ (see Ref. 6). Fig. 9 clearly demonstrates that this existing increase is nonetheless weaker than the increase of the efficiency of scattering in energy. However, it is worth noting too that the increase of L also results in a widening of the α_0 -range where resonant interaction is possible.⁶ As a result, the α_0 -range such that $E_{\parallel 0}^* < 100$ mV/m is actually increased at larger L -shells.

A comparison of the right and left panels in Fig. 9 shows that the value of the normalized wave frequency does not influence significantly the relationship between nonlinear acceleration and scattering levels. This (absence of) effect can be explained by the fact that the wave phase velocity $v_R = \omega/k_{\parallel}$ is independent of the wave frequency for waves propagating at (or near to) the Gendrin angle ($k_{\parallel} \sim \omega$). For much more oblique waves propagating close to the resonance-cone angle ($k_{\parallel} \sim \omega^2$, see Ref. 1), we expect a stronger dependence of all system parameters (including $E_{\parallel 0}^*$) on the wave frequency.

VI. DISCUSSION AND CONCLUSIONS

In this paper, we consider electron resonant interaction with high-amplitude oblique whistler waves propagating in an inhomogeneous magnetic field. More specifically, we compare two different effects of wave-particle interaction: scattering and nonlinear trapping. The latter one can lead to a very strong acceleration of individual particles, but the corresponding probability of trapping is small. As a result, a weak energy scattering of particles by the waves may be more effective than acceleration due to trapping even for high-amplitude waves. Thus, the presence of high amplitude waves does not necessarily imply a nondiffusive character of wave-particle interactions. Previous estimates usually give threshold values for the wave amplitude such that trapping becomes possible^{1,9,42} but as we have shown, even for high amplitude waves, only over certain energy and pitch-angle ranges does nonlinear acceleration by trapping really become more effective than scattering. In case of whistler-mode waves with amplitudes ~ 50 – 100 mV/m and propagation in the quasi-electrostatic mode for energies $\in [30, 100]$ keV, the α_0 -range of prevalence of nonlinear acceleration is rather narrow $\sim 5^\circ$ – 10° . This range is much wider for small energy electrons ~ 10 keV.

It is interesting to note that the amplitude of regular energy jumps $\langle \Delta\gamma \rangle \sim \Upsilon_0$ and the probability of trapping Π depend similarly on the small parameter $1/k_0$. Thus, the ratio of energy gained by particles due to trapping $\Delta E_{\text{gain}} \sim \Pi \Delta\gamma_{\text{trap}}$ and lost by particles due to scattering $\Delta E_{\text{lost}} \sim (1 - \Pi) \langle \Delta\gamma \rangle$ are of the same order: for $1/k_0 \ll 1$ the ratio $\Delta E_{\text{lost}}/\Delta E_{\text{gain}}$ depends on k_0 only through the combination $\epsilon k_0 \sim 1$. Such a relationship between lost and gained energies was shown before in Ref. 44.

In this paper, we show that for high-amplitude oblique waves, the process of particle scattering is substantially modified in comparison with particle interaction with low-amplitude oblique waves in the quasi-linear regime. Even if the probability of trapping is small (or even zero, e.g., for $\partial S/\partial z < 0$) the evolution of the particle energy due to scattering does not keep a diffusive character. There is a nonzero average value of the energy jumps $\langle \Delta\gamma \rangle \neq 0$. For long term dynamics, such jumps can be more important than diffusion due to $\text{Var}(\Delta\gamma)$. They are responsible for a particle drift in energy space¹⁷ with a velocity $\dot{\gamma} \approx \langle \Delta\gamma \rangle / T_{\text{bounce}}$, where T_{bounce} is the bounce period. For 100 keV particles with $\alpha_0 \sim 45^\circ$ and 50 mV/m wave amplitude, we can estimate this velocity as $\dot{\gamma} \approx -2$ keV/s. This effect can be important for electron deceleration and related wave amplification (see discussion in

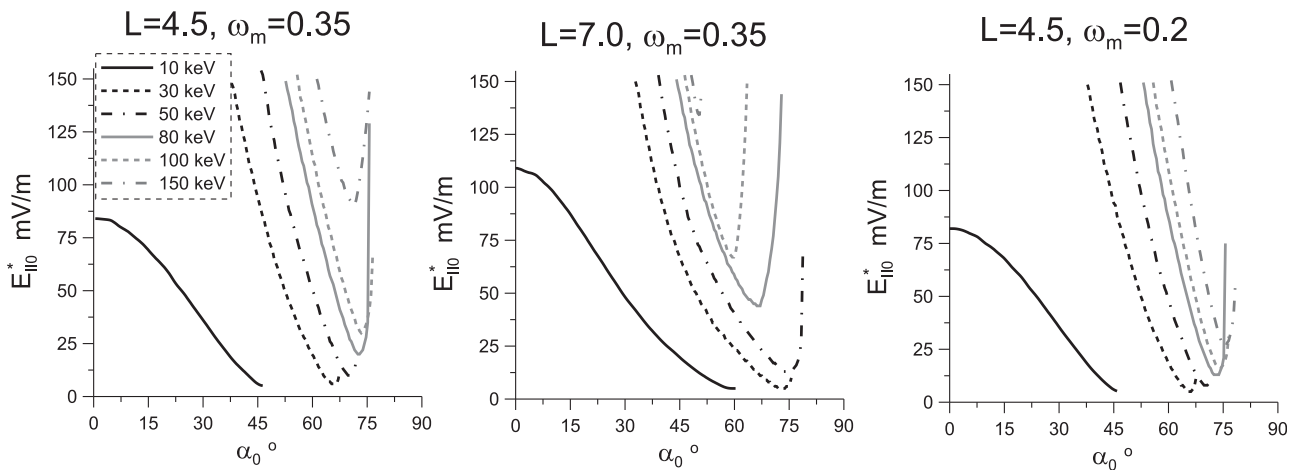


FIG. 9. The critical wave amplitude is shown as a function of pitch-angle for several energies and three sets of system parameters.

Ref. 31). The problem of nonlinear wave generation and amplification^{36,46,51} is very important for the planetary radiation belts, because purely linear instabilities seem to be unable to generate the observed high-amplitude waves.^{47,52}

For ~ 100 keV electrons at $L \sim 5$, this effect has the same magnitude for 50 mV/m oblique whistler-mode waves as deceleration by phase bunching due to cyclotron-resonant interaction with high-amplitude (~ 60 pT) parallel whistler-mode waves,² but it should become stronger at lower energies, where it affects electrons with smaller equatorial pitch-angles $\alpha_0 < 45^\circ$. Since it acts against electron precipitation in the loss-cone (at very low α_0), its coexistence at low electron energy with trapping acceleration could allow multiple (successive) accelerations before actual precipitation eventually occurs.⁵

In conclusion, we have investigated the nonlinear scattering in energy of electrons resonantly interacting with high-amplitude oblique whistler-mode waves. A comparison of the efficiency of energy scattering and nonlinear acceleration by trapping shows that for reasonable wave amplitudes and electron energies < 100 keV, there is always some range of equatorial pitch-angles where nonlinear trapping prevails. This range is rather wide for small energy electrons ~ 10 keV but it shrinks as energy increases. We have derived analytical equations for the energy jumps due to nonlinear scattering. These expressions are valid for any system with inhomogeneous magnetic field and quasi-electrostatic waves.

ACKNOWLEDGMENTS

Work of A.A.V. was supported by Grant No. MK-1781.2014.2. Work of V.A.A. was supported by Russian Fund of Basic Research (Project No. 13-01-00251). Work by O.A. was performed under JHU/APL Contract No. 922613 (RBSP-EFW). Work of K.V.V. was supported through CNES by grant (Modele d'ondes).

¹O. Agapitov, A. Artemyev, D. Mourenas, V. Krasnoselskikh, J. Bonnell, O. Le Contel, C. M. Cully, and V. Angelopoulos, *J. Geophys. Res.* **119**, 1608–1626, doi:10.1002/2013JA019223 (2014).

²J. M. Albert, *Geophys. Res. Lett.* **29**, 1275, doi:10.1029/2001GL013941 (2002).

³J. M. Albert, X. Tao, and J. Bortnik, “Aspects of nonlinear wave-particle interactions,” in *Dynamics of the Earth's Radiation Belts and Inner*

Magnetosphere, edited by D. Summers, I. U. Mann, D. N. Baker, and M. Schulz (American Geophysical Union, 2013).

⁴V. I. Arnold, V. V. Kozlov, and A. I. Neishtadt, *Mathematical Aspects of Classical and Celestial Mechanics*, 3rd ed., Dynamical Systems III, Encyclopedia of Mathematical Sciences (Springer-Verlag, New York, 2006).

⁵A. Artemyev, V. Krasnoselskikh, O. Agapitov, D. Mourenas, and G. Rolland, *Phys. Plasmas* **19**, 122901 (2012).

⁶A. V. Artemyev, A. A. Vasiliev, D. Mourenas, O. Agapitov, and V. Krasnoselskikh, *Phys. Plasmas* **20**, 122901 (2013).

⁷A. V. Artemyev, A. A. Vasiliev, D. Mourenas, O. Agapitov, V. Krasnoselskikh, D. Boscher, and G. Rolland, *Geophys. Res. Lett.* **41**, 5727–5733, doi:10.1002/2014GL061380 (2014).

⁸T. F. Bell, *J. Geophys. Res.* **89**, 905–918, doi:10.1029/JA089iA02p00905 (1984).

⁹T. F. Bell, *J. Geophys. Res.* **91**, 4365–4379, doi:10.1029/JA091iA04p04365 (1986).

¹⁰T. F. Bell and U. S. Inan, *J. Geophys. Res.* **86**, 9047–9063, doi:10.1029/JA086iA11p09047 (1981).

¹¹J. Bortnik, R. M. Thorne, and U. S. Inan, *Geophys. Res. Lett.* **35**, L21102, doi:10.1029/2008GL035500 (2008).

¹²C. Cattell, J. R. Wygant, K. Goetz, K. Kersten, P. J. Kellogg, T. von Rosenvinge, S. D. Bale, I. Roth, M. Temerin, M. K. Hudson, R. A. Mewaldt, M. Wiedenbeck, M. Maksimovic, R. Ergun, M. Acuna, and C. T. Russell, *Geophys. Res. Lett.* **35**, L01105, doi:10.1029/2007GL032009 (2008).

¹³C. M. Cully, J. W. Bonnell, and R. E. Ergun, *Geophys. Res. Lett.* **35**, L17S16, doi:10.1029/2008GL033643 (2008).

¹⁴A. G. Demekhov, V. Y. Trakhtengerts, M. J. Rycroft, and D. Nunn, *Geomag. Aeron.* **46**, 711–716 (2006).

¹⁵A. G. Demekhov, V. Y. Trakhtengerts, M. J. Rycroft, and D. Nunn, *Geomag. Aeron.* **49**, 24–29 (2009).

¹⁶X. Deng, M. Ashour-Abdalla, M. Zhou, R. Walker, M. El-Alaoui, V. Angelopoulos, R. E. Ergun, and D. Schriver, *J. Geophys. Res.* **115**, A09225, doi:10.1029/2009JA015107 (2010).

¹⁷D. Dolgopyat, “Repulsion from resonances,” *Memoires De La Societe Mathematique De France* (Société Mathématique de France, 2012), Vol. 128.

¹⁸W. E. Drummond and D. Pines, *Nucl. Fusion* **5**(Suppl. 3), 1049–1058 (1962).

¹⁹K. B. Dysthe, *J. Geophys. Res.* **76**, 6915–6931, doi:10.1029/JA076i028p06915 (1971).

²⁰R. E. Ergun, D. M. Malaspina, I. H. Cairns, M. V. Goldman, D. L. Newman, P. A. Robinson, S. Eriksson, J. L. Bougeret, C. Briand, S. D. Bale, C. A. Cattell, P. J. Kellogg, and M. L. Kaiser, *Phys. Rev. Lett.* **101**(5), 051101 (2008).

²¹A. J. Hull, L. Muschietti, M. Oka, D. E. Larson, F. S. Mozer, C. C. Chaston, J. W. Bonnell, and G. B. Hospodarsky, *J. Geophys. Res.* **117**, 12104, doi:10.1029/2012JA017870 (2012).

²²A. P. Itin, A. I. Neishtadt, and A. A. Vasiliev, *Phys. D* **141**, 281–296 (2000).

²³V. I. Karpman, J. N. Istomin, and D. R. Shklyar, *Plasma Phys.* **16**, 685–703 (1974).

²⁴V. I. Karpman and D. R. Shklyar, *Sov. JETP* **35**, 500 (1972).

²⁵C. F. Kennel and F. Engelmann, *Phys. Fluids* **9**, 2377–2388 (1966).

²⁶C. F. Kennel and H. E. Petschek, *J. Geophys. Res.* **71**, 1–28, doi:10.1029/JZ071i001p00001 (1966).

- ²⁷Y. V. Khotyaintsev, C. M. Cully, A. Vaivads, M. André, and C. J. Owen, *Phys. Rev. Lett.* **106**(16), 165001 (2011).
- ²⁸C. Krafft, A. S. Volokitin, and V. V. Krasnoselskikh, *Astrophys. J.* **778**, 111 (2013).
- ²⁹O. Le Contel, A. Roux, C. Jacquey, P. Robert, M. Berthomier, T. Chust, B. Grison, V. Angelopoulos, D. Sibeck, C. C. Chaston, C. M. Cully, B. Ergun, K.-H. Glassmeier, U. Auster, J. McFadden, C. Carlson, D. Larson, J. W. Bonnell, S. Mende, C. T. Russell, E. Donovan, I. Mann, and H. Singer, *Ann. Geophys.* **27**, 2259–2275 (2009).
- ³⁰W. Li, R. M. Thorne, J. Bortnik, Y. Y. Shprits, Y. Nishimura, V. Angelopoulos, C. Chaston, O. Le Contel, and J. W. Bonnell, *Geophys. Res. Lett.* **38**, 14103, doi:10.1029/2011GL047925 (2011).
- ³¹D. Mourenas, A. V. Artemyev, O. V. Agapitov, and V. Krasnoselskikh, *J. Geophys. Res.* **119**, 2775–2796, doi:10.1002/2013JA019674 (2014).
- ³²A. I. Neishtadt, *Hamiltonian Systems with Three or More Degrees of Freedom*, NATO ASI Series, edited by C. Dordrecht (Kluwer Academic Publishers, 1999), Vol. 533, pp. 193–213.
- ³³A. I. Neishtadt and A. A. Vasiliev, *Nucl. Instrum. Methods Phys. Res., Sect. A* **561**, 158–165 (2006).
- ³⁴D. Nunn, *J. Plasma Phys.* **6**, 291 (1971).
- ³⁵Y. Omura, N. Furuya, and D. Summers, *J. Geophys. Res.* **112**, 6236, doi:10.1029/2006JA012243 (2007).
- ³⁶Y. Omura, Y. Katoh, and D. Summers, *J. Geophys. Res.* **113**, 4223, doi:10.1029/2007JA012622 (2008).
- ³⁷Y. Omura, H. Matsumoto, D. Nunn, and M. J. Rycroft, *J. Atmos. Terr. Phys.* **53**, 351–368 (1991).
- ³⁸A. Osmane and A. M. Hamza, *Phys. Rev. E* **85**(5), 056410 (2012).
- ³⁹A. Osmane and A. M. Hamza, *Nonlinear Processes Geophys.* **21**, 115–125 (2014).
- ⁴⁰E. V. Panov, A. V. Artemyev, W. Baumjohann, R. Nakamura, and V. Angelopoulos, *J. Geophys. Res.* **118**, 3065–3076, doi:10.1002/jgra.50203 (2013).
- ⁴¹B. W. Sheeley, M. B. Moldwin, H. K. Rassoul, and R. R. Anderson, *J. Geophys. Res.* **106**, 25631–25642, doi:10.1029/2000JA000286 (2001).
- ⁴²D. Shklyar and H. Matsumoto, *Surv. Geophys.* **30**, 55–104 (2009).
- ⁴³D. R. Shklyar, *Sov. Phys. JETP* **53**, 1197–1192 (1981).
- ⁴⁴D. R. Shklyar, *Ann. Geophys.* **29**, 1179–1188 (2011).
- ⁴⁵Y. Y. Shprits, D. A. Subbotin, N. P. Meredith, and S. R. Elkington, *J. Atmos. Sol. Terr. Phys.* **70**, 1694–1713 (2008).
- ⁴⁶D. Summers, R. Tang, and Y. Omura, *J. Geophys. Res.* **116**, A10226, doi:10.1029/2011JA016602 (2011).
- ⁴⁷D. Summers, R. Tang, and R. M. Thorne, *J. Geophys. Res.* **114**, A10210, doi:10.1029/2009JA014428 (2009).
- ⁴⁸X. Tao and J. Bortnik, *Nonlinear Processes Geophys.* **17**, 599–604 (2010).
- ⁴⁹X. Tao, J. Bortnik, R. M. Thorne, J. M. Albert, and W. Li, *Geophys. Res. Lett.* **39**, L06102, doi:10.1029/2012GL051202 (2012).
- ⁵⁰V. Y. Trakhtengerts, *Geomag. Aeron.* **6**, 827–836 (1966).
- ⁵¹V. Y. Trakhtengerts, *Ann. Geophys.* **17**, 95–100 (1999).
- ⁵²V. Y. Trakhtengerts, A. G. Demekhov, E. E. Titova, B. V. Kozelov, O. Santolik, D. Gurnett, and M. Parrot, *Phys. Plasmas* **11**, 1345–1351 (2004).
- ⁵³V. Y. Trakhtengerts and M. J. Rycroft, *Whistler and Alfvén Mode Cyclotron Masers in Space* (Cambridge University Press, 2008).
- ⁵⁴B. T. Tsurutani, G. S. Lakhina, and O. P. Verkhoglyadova, *J. Geophys. Res.* **118**, 2296–2312, doi:10.1002/jgra.50264 (2013).
- ⁵⁵A. A. Vedenov, E. Velikhov, and R. Sagdeev, *Nucl. Fusion* **2**(Suppl. 2), 465–475 (1962).
- ⁵⁶P. Veltri and G. Zimbardo, *J. Geophys. Res.* **98**, 13335–13346, doi:10.1029/93JA01144 (1993).
- ⁵⁷L. B. Wilson, A. Koval, A. Szabo, A. Breneman, C. A. Cattell, K. Goetz, P. J. Kellogg, K. Kersten, J. C. Kasper, B. A. Maruca, and M. Pulupa, *J. Geophys. Res.* **118**, 5–16, doi:10.1029/2012JA018167 (2013).
- ⁵⁸Y. Zhang, H. Matsumoto, H. Kojima, and Y. Omura, *J. Geophys. Res.* **104**, 449–462, doi:10.1029/1998JA900049 (1999).